

1
2
3
4
5
6
7
8
9
10
11
12
13
14
15
16
17
18
19
20
21
22
23
24
25
26
27
28
29
30
31
32
33
34
35

Responses of globally important phytoplankton groups to olivine dissolution products and implications for carbon dioxide removal via ocean alkalinity enhancement

David A. Hutchins^{1†*}, Fei-Xue Fu¹, Shun-Chung Yang¹, Seth G. John¹, Stephen J. Romaniello²,
M. Grace Andrews², Nathan G. Walworth^{1,2,3†*}

¹University of Southern California, Los Angeles, CA, USA

²Vesta, PBC, San Francisco, CA, USA

³J. Craig Venter Institute, La Jolla, CA, USA

†These authors contributed equally to this work

*Correspondence: David A. Hutchins - dahutch@usc.edu, Nathan G. Walworth – nate@vesta.earth

36

37 **Abstract**

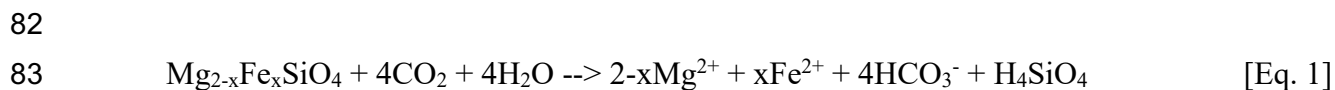
38

39 Anthropogenic greenhouse gas emissions are leading to global temperature increases,
40 ocean acidification, and significant ecosystem impacts. Given current emissions trajectories, the
41 IPCC calls for both the rapid abatement of CO₂ emissions and development of carbon dioxide
42 removal (CDR) strategies that can address legacy emissions and difficult to abate emissions
43 sources. These CDR methods must efficiently and safely sequester gigatons of atmospheric CO₂.
44 Coastal Enhanced Weathering (CEW) via the addition of the common mineral olivine to coastal
45 waters is one promising approach to enhance ocean alkalinity for large-scale CDR. As olivine
46 weathers, it releases several biologically active dissolution products, including alkalinity, trace
47 metals, and the nutrient silicate. Released trace metals can serve as micronutrients but may also
48 be toxic at high concentrations to marine biota including phytoplankton that lie at the base of
49 marine food webs. We grew several globally important phytoplankton functional groups under
50 elevated concentrations of olivine dissolution products using a synthetic olivine leachate (OL)
51 based on olivine elemental composition, and monitored their physiological and biogeochemical
52 responses. This allowed us to determine physiological impacts and thresholds at elevated olivine
53 leachate concentrations, in addition to individual effects of specific constituents. We found both
54 positive and neutral responses but no evident toxic effects for two silicifying diatoms, a
55 calcifying coccolithophore, and three cyanobacteria. In both single and competitive co-cultures,
56 silicifiers and calcifiers benefited from olivine dissolution products like iron and silicate or
57 enhanced alkalinity, respectively. The non-N₂-fixing picocyanobacterium could use synthetic
58 olivine-derived iron for growth, while N₂-fixing cyanobacteria could not. However, other trace
59 metals like nickel and cobalt supported cyanobacterial growth across both groups. Growth
60 benefits to particular phytoplankton groups *in situ* will depend on species-specific responses and
61 ambient concentrations of other required nutrients. Results suggest olivine dissolution products
62 appear unlikely to cause negative effects for marine phytoplankton, even at high concentrations,
63 and may support growth of particular taxa under some conditions. Future studies can shed light
64 on long-term evolutionary responses to olivine exposure, and on the potential effects that marine
65 microbes may in turn have on olivine dissolution rates and regional biogeochemistry.

66

67 Introduction

68
69 Excess anthropogenic greenhouse gas emissions are driving global changes to Earth
70 systems and leading to simultaneous increases in sea surface temperatures, ocean acidification,
71 and regional shifts in nutrient supplies (Bach et al., 2019). To counteract these trends and limit
72 the average global temperature increase to 1.5-2°C, carbon dioxide removal (CDR) methods that
73 can collectively remove and permanently store gigatons of atmospheric CO₂ (GtCO₂) must be
74 developed (Renforth and Henderson, 2017). Coastal Enhanced Weathering (CEW) with olivine
75 (Mg_{2-x}Fe_xSiO₄) has been proposed as an economically scalable form of ocean alkalinity
76 enhancement (OAE), as it is a globally abundant, naturally occurring ultramafic silicate mineral
77 (Bach et al., 2019; Beerling et al., 2021). Olivine is considered to be one of the most favorable
78 minerals for CDR as it weathers quickly under Earth surface conditions (Renforth and
79 Henderson, 2017; Hartmann et al., 2013; Rimstidt et al., 2012). Similar to other silicate minerals,
80 it dissolves in water to release cations (Mg²⁺, Fe²⁺) and generates alkalinity (principally HCO₃⁻),
81 with up to 4 mol of CO₂ sequestered per mol of olivine [Eq. 1].



85 Forsteritic olivine is the magnesium-rich end-member of olivine and can contain various other
86 trace constituents. For example, olivine used in this study contains ~92% magnesium (Mg²⁺) and
87 ~8% ferrous iron (Fe²⁺) along with trace amounts (<1%) of other metals such as nickel (Ni),
88 chromium (Cr), and cobalt (Co). As olivine weathers, it releases several biologically important
89 dissolution products into the surrounding seawater: (I) bicarbonate (HCO₃⁻) and carbonate ion
90 (CO₃²⁻), hereafter summarized as “alkalinity”; (II) silicic acid (Si(OH)₄) hereafter termed
91 silicate; (III) and a variety of trace metals including iron (Fe²⁺, or oxidized aqueous species),
92 nickel (Ni²⁺), cobalt (Co²⁺), and chromium (CrVI). These dissolution products have the potential
93 to affect important phytoplankton functional groups like silicifying algae (diatoms), calcifying
94 algae (coccolithophores), and cyanobacteria, which lie at the base of marine food webs and drive
95 the biological carbon pump (Moran, 2015). Hence, it is important to understand the specific
96 effects of these constituents on globally important phytoplankton groups, particularly at elevated
97 concentrations to simulate large-scale CEW applications.

98 Significant alkalinity additions from olivine weathering can consume CO₂ from the
99 surrounding seawater, causing a CO₂ deficit until air-sea equilibration. This shift in the carbonate
100 system from CO₂ to HCO₃⁻/CO₃²⁻ by transient, non-equilibrated OAE will affect phytoplankton
101 functional groups differently, with some taxa being more sensitive than others. For example, it is
102 predicted that calcifying organisms like coccolithophores may benefit from CEW due to
103 decreases in proton concentrations (H⁺) and increases in the CaCO₃ saturation state.
104 Additionally, dissolving one mole of olivine leads to a one mole increase in dissolved silicate,
105 which is an essential and often bio-limiting nutrient for silicifying organisms like diatoms, a
106 phytoplankton group estimated to contribute up to 40% of the marine primary production

107 (Bertrand et al., 2012). Hence, diatoms may especially benefit from CEW applications with
108 olivine. Additionally, diatoms are particularly noted for being dominant phytoplankton in the
109 coastal regimes where olivine deployments are likely to take place (Field et al., 1998). While
110 there are both planktonic and benthic species of diatoms, the latter will presumably be exposed to
111 especially sustained and elevated levels of dissolution products when olivine is deployed in
112 natural marine sediments. It is unknown if either group, calcifiers or silicifiers, may consistently
113 outcompete the other following CEW with olivine (Bach et al., 2019).

114 Trace metals like Fe and Ni are general micronutrients required by all classes of
115 phytoplankton, and could potentially support their growth upon fluxes into seawater from olivine
116 weathering. In particular, dinitrogen (N₂)-fixing cyanobacteria and diatoms both have elevated
117 Fe requirements (Hutchins and Sañudo-Wilhelmy, 2021; Hutchins and Boyd, 2016), and so may
118 stand to benefit from increases in Fe concentrations. Although a required micronutrient at low
119 levels, in high enough concentrations Ni may potentially negatively impact phytoplankton
120 growth, although one recent study showed limited to no toxic effects of very high Ni
121 concentrations (e.g. 50,000 nmol L⁻¹) for several phytoplankton taxa (Guo et al., 2022). Cobalt
122 can also serve as a micronutrient for phytoplankton (Sunda and Huntsman, 1995; Hawco et al.,
123 2020) but may also be toxic at high concentrations (Karthikeyan et al., 2019). However, other
124 trace metals found with olivine such as Cr are not nutrient elements and also need to be
125 considered in terms of their possible toxicity to phytoplankton (Flipkens et al., 2021; Frey et al.,
126 1983).

127 Hence, it is important to understand the taxon-specific effects of these constituents to
128 determine thresholds at which key phytoplankton functional groups may experience positive or
129 negative effects. Furthermore, it is important to expose phytoplankton to elevated concentrations
130 of olivine dissolution products simultaneously to understand what impacts may occur for large
131 CEW applications. Exposures of organisms to concentrated olivine dissolution products also
132 provides an “worst case scenario” benchmark, which can be compared to lower actual
133 environmental exposures resulting from small CEW additions, slower olivine dissolution time
134 scales, and dilution from advection. While olivine weathers relatively quickly compared to other
135 silicate minerals (Hartmann et al., 2013), dissolution of olivine grains is gradual (i.e. years)
136 relative to microbial physiological responses (hours), posing a challenge to test different
137 concentrations of olivine constituents on phytoplankton physiology. To address this, we prepared
138 a synthetic olivine leachate (OL) composed of olivine dissolution products with trace metal
139 concentrations well over those of seawater (17-12,000 times higher), in order to represent a
140 “worst case” scenario for a CEW project. This scenario was estimated based on the maximum
141 expected impact of olivine weathering on the chemistry of the overlying water column.
142 Assuming a 10 cm thick layer of pure olivine sand dissolves with a 100 year half-life dissolving
143 into 1 meter of overlying water with a 24 hour residence time, the anticipated steady state change
144 in the alkalinity of the overlying water column is 65 umol/kg (assuming 4 moles of alkalinity per
145 mole olivine (Meysman and Montserrat, 2017) and 100% release to the water column). The
146 concentrations of other components were chosen assuming stoichiometric congruent dissolution

147 and quantitative release to the water column as well -- a worst case scenario. Furthermore,
148 phytoplankton were exposed to OL within a small, enclosed batch culture. We cultured 6 species
149 representing three globally important phytoplankton functional groups: 2 diatoms (*Nitzschia*,
150 *Ditylum*), 1 coccolithophore (*Emiliana*), 2 dinitrogen (N₂) fixing cyanobacteria (*Trichodesmium*,
151 *Crocospaera*), and 1 non-N₂ fixing picocyanobacterium (*Synechococcus*). All of these species
152 are planktonic, with the exception of the diatom *Nitzschia* which frequently forms benthic
153 biofilms (Yamamoto et al., 2008). Cultures were grown semi-continuously in natural seawater
154 based modified Aquil media (Sunda et al., 2005) with OL as the only available Fe source (and Si
155 source for diatoms). For all experiments, cultures were sampled for a basic set of core
156 biogeochemical and physiological parameters (Fu et al., 2005, 2008; Tovar-Sanchez et al., 2003;
157 Paasche et al., 1996). This approach allowed us to compare and contrast phytoplankton taxon-
158 specific responses, including: **1**) physiological impacts at extremely high OL concentrations, **2**)
159 physiological thresholds and dose responses across a range of increasing concentrations of OL,
160 and **3**) individual effects of specific OL constituents.

161

162 **Materials and Methods**

163

164 *Culture growth conditions and experimental set up*

165

166 Six species of phytoplankton were used in these experiments, including two diatoms, *Ditylum*
167 (centric, planktonic) and *Nitzschia* (pennate, benthic), one coccolithophore, *Emiliana huxleyi*,
168 one picoplanktonic cyanobacterium (*Synechococcus*), and two marine dinitrogen (N₂) fixing
169 cyanobacteria, *Trichodesmium* IMS 101 and *Crocospaera* WH 0005. Cultures were grown in
170 500 mL polycarbonate flasks at 28⁰C for the three cyanobacteria, and 20⁰C for the diatoms and
171 *Emiliana huxleyi*. Cool-white fluorescent light was supplied following a 12:12 light:dark cycle
172 at an irradiance level of 150 μEm⁻²s⁻¹. Stock cultures were grown in natural offshore seawater
173 collected with trace metal clean methods (John et al., 2022), which was used to make modified
174 Aquil control medium (ACM) (Sunda et al., 2005). For experiments, cultures were inoculated
175 into the three treatments described below with the addition of 4μM phosphate (PO₄³⁻) and 60 μM
176 nitrate (NO₃⁻). There was no nitrogen (N) added into the Aquil medium for the N₂ fixers. Iron,
177 Cobalt, Nickel (Fe, Co and Ni, required by all species) and silicate (SiOH₄, required by diatoms
178 only) were not added to the Aquil medium, except as components of the olivine leachate (see
179 below). The background nutrient concentrations in the collected natural seawater were 1μM
180 NO₃⁻, 0.1μM PO₄³⁻ and 3μM SiOH₄.

181

182 *Synthetic olivine leachate preparation*

183

184 To simulate acute exposure of phytoplankton to elevated levels of olivine dissolution products in
185 seawater, we prepared an artificial concentrated OL stock solution based on elemental analyses
186 of commercial ground olivine rock (Sibelco. (2022) Technical Data - Olivine Refractory Grade

187 Fine. Antwerp, Belgium). For experimental exposures, this concentrated OL stock was added to
 188 seawater growth medium to yield the final concentrations shown in **Table 1**, which will be
 189 referred to throughout as a “100%” concentration of OL. Experiments examining biological
 190 effects across a dilution range (0-100%) used correspondingly lower additions of the
 191 concentrated stock. The only other components added to the OL were the major nutrients nitrate
 192 (60 μM NO_3^-) and phosphate (4 μM PO_4^{3-}). These are required nutrients for growth of
 193 phytoplankton, and were added at the same concentration to the OL and the Aquil control
 194 medium. For experiments with N_2 -fixing cyanobacteria, nitrate was omitted and phosphate was
 195 the only nutrient added.

196
 197 **Table 1.** Concentrations of added ions or compounds in serial dilutions of synthetic olivine leachate (OL, 0% to
 198 100%) used in the phytoplankton growth experiments; and concentrations of components in the three concentrated
 199 stocks used to prepare experimental medium (1mL/L added for 100% OL). Stock C was prepared in 10 nM HCl to
 200 keep the trace metals in solution until addition.

Concentration added to growth medium	OL Added	Mg^{2+} (μM)	SiOH_4 (μM)	OH^- (μM)	Fe(II) (μM)	Ni(II) (μM)	Cr(VI) (μM)	Co(II) (μM)
100%		44.9	25	100	3.36	0.13	0.12	0.006
80%		35.9	20	80	2.7	0.10	0.10	0.005
50%		22.5	12.3	50	1.7	0.07	0.06	0.003
30%		13.5	7.5	30	1.0	0.04	0.04	0.002
10%		4.5	2.5	10	0.34	0.01	0.01	0.001
0%		0	0	0	0	0	0	0
Concentrated stock solutions (mM)		MgCl_2	NaSiO_2	NaOH	FeCl_2	NiCl_2	K_2CrO_4	CoCl_2
Stock A		44.9						
Stock B			25	100				
Stock C					3.36	0.13	0.12	0.006

201
 202 *Experimental methods*
 203
 204 Semi-continuous culturing methods were used to achieve nearly steady-state growth. Cultures
 205 were diluted with fresh medium every 2 or 3 days, using in vivo fluorescence as a real time
 206 biomass indicator. Dilutions were calculated to bring the cultures back down to the biomass
 207 levels that were recorded after the previous day’s dilution. In this way, cultures were allowed to
 208 determine their own growth rates under each set of experimental conditions, without ever nearing
 209 stationary phase, significantly depleting nutrients or self-shading (Fu et al., 2022). For all
 210 experiments, cultures were sampled for a basic set of core biomass and physiological parameters,
 211 including cell counts, CO_2 fixation, particulate organic carbon (POC), particulate organic
 212 nitrogen (PON), particulate organic phosphorus (POP) and biogenic silica (BSi, diatoms only)
 213 once steady-state growth was obtained for each growth condition (typically after 8–10

214 generations). Steady-state growth status was defined as no significant difference in cell- or in
215 vivo-specific growth rates for at least 3 consecutive transfers.

216

217 There were four sets of experiments in this project:

218

219 *1) Acute responses to elevated olivine leachate levels.* The goal of this set of experiments was to
220 investigate the responses of the diatoms *Nitzschia* and *Ditylum* to relatively high concentrations
221 of olivine leachate, in order to determine acute exposure responses. To see if the leachate may
222 have a positive or negative effect on their physiology, they were compared to their respective
223 control cultures. There were a total of three treatments consisting of: OL (100%), ACM, and
224 ACM with low Fe/Si (with 2 nM Fe EDTA added, and no added SiOH₄).

225

226 *2) Responses to a broad range of olivine leachate levels.* In these experiments, *Synechococcus*,
227 *Crocospaera*, *Ditylum*, and *Emiliania huxleyi* were grown in culture medium across a series of
228 OL dilutions (Table 1) to determine their responses across a range of leachate concentrations,
229 from high to very low-level exposures.

230

231 *3) Fe bioavailability and Cr toxicity from olivine leachate to N₂-fixing cyanobacteria.* The goal
232 of this set of experiments was to investigate OL-derived Fe bioavailability to N₂-fixing
233 cyanobacteria, *Trichodesmium* and *Crocospaera*. An additional experiment was conducted to
234 investigate potential Cr(VI) toxicity.

235

236 *4) Two species co-culture competition experiments during olivine leachate exposure.* In order to
237 test how OL may affect co-existence and competition between the diatom *Ditylum* and the
238 coccolithophore *Emiliania huxleyi*, a simple batch co-culture competition experiment was carried
239 out in which the 2 species were inoculated at a 1:1 ratio (based on equivalent levels of cellular
240 Chlorophyll a due to the large differences in their cell sizes) into 100% OL and regular ACM,
241 and grown for 10 days until early stationary phase. In vivo fluorescence and cell counts were
242 monitored daily. Relative abundance and growth rates of the two species were determined based
243 on microscopic cell counts during the exponential growth phase of the mixed cultures. Biogenic
244 silica (BSi, an indicator of diatom abundance) and particulate inorganic carbon (PIC or calcite,
245 an indicator of coccolithophore abundance) were collected every other day in order to further
246 determine how these two species responded to co-culture with and without leachate additions.

247

248 *Analytical methods*

249

250 *Determination of growth rates and chlorophyll a* Growth rates were determined based on both
251 microscopic cell counts and chlorophyll a. For chlorophyll a determination, subsamples of 30 ml
252 from each triplicate bottle were GF/F filtered, extracted in 6 ml of 90% acetone, stored overnight
253 in the dark at -20°C, and chlorophyll a concentrations were measured fluorometrically using a

254 Turner 10-AU fluorometer (Welschmeyer, 1994). Specific growth rates were determined using
255 the equation:

256
257
$$\mu = \frac{\ln\left(\frac{N_{T_{final}}}{N_{T_{initial}}}\right)}{T_{final} - T_{initial}}$$

258

259 where μ is the specific growth rate (per day) and N is the chlorophyll a concentration at $T_{initial}$
260 and T_{final} (Kling et al., 2021).

261
262 Particulate C, N, P and Si. Particulate organic carbon and nitrogen (CHN) samples from all
263 experiments were filtered (pre-combusted GF/F) and frozen for analysis using a Costech
264 Elemental Analyzer (Hutchins et al., 2007). Samples for biogenic silica (BSi) were analyzed
265 according to (Brzezinski, 1985). POP (particulate organic phosphorus) samples were collected
266 onto pre-combusted 25 mm GF/F filters and analyzed as in Fu et al. 2005 (Fu et al., 2005).

267
268 Primary productivity. For all species other than the coccolithophore (see below), primary
269 production was measured in triplicate using 24h incubations (approximating net PP) with
270 $H^{14}CO_3$ under the appropriate experimental growth conditions for each treatment (Fu et al.,
271 2008). CO_2 fixation rates were calculated using measured final experimental DIC concentrations
272 and biomass. All samples for primary production were counted using a Wallac System 1400
273 liquid scintillation counter.

274
275 Photosynthetic and calcification rates of *Emiliana huxleyi*. For the coccolithophore, two 40 mL
276 subsamples from each triplicate bottle were spiked with 0.5 μCi $NaH^{14}CO_3$. One subsample was
277 incubated in the light and the other in the dark for 24 h. Then two sets of 20 mL aliquots from
278 each sub- sample were filtered onto Whatman GF/F filters. The filters for photosynthetic rate
279 determination were fumed with saturated HCl before adding scintillation cocktail fluid.
280 Photosynthetic rate and calcification rate were calculated as described in Paasche et al. 1996
281 (Paasche et al., 1996).

282
283 Fe quota. Intracellular Fe content was determined by filtering culture samples onto acid-washed
284 0.2- μm polycarbonate filters (Millipore), and rinsing with oxalate reagent to remove extracellular
285 trace metals (Tovar-Sanchez et al., 2003). Fe was determined with a magnetic sector-field high-
286 resolution inductively coupled plasma mass spectrometer (ICPMS) (Element 2, Thermo) (Jiang
287 et al., 2018; John et al., 2022).

288
289 Statistical methods. A one-way ANOVA analysis of variance was used to analyze differences
290 between treatments using Prism 8. Differences between treatments were considered significant at
291 $p < 0.05$. Post-hoc comparisons were conducted using the Tukey's multiple comparison test to
292 determine any pairwise differences.

293

294 Results

295

296 Diatoms

297 We hypothesized that diatoms may benefit from the OL products Si and Fe, as they are
298 both required for growth and can be limiting for this group (Tréguer et al., 2018). Hence, we
299 grew the benthic diatom *Nitzschia* across three treatments: OL alone, Aquil control medium
300 (ACM), and ACM but with low, limiting Si and Fe concentrations (ACM-low-SF). *Nitzschia*
301 grew and fixed carbon just as well in the OL as the ACM ($p=0.35$; $p=0.21$), while showing
302 reduced rates in the ACM-low-SF treatment ($p=0.02$; $p<0.0001$; **Fig. 1A, B**). Likewise, the
303 particulate Si:C ratios demonstrated OL to be just as good a source of Si to *Nitzschia* as the ACM
304 ($p=0.98$), and considerably better than the ACM-low-SF ($p=0.0012$; **Fig. 1C**).

305 Growth and CO₂ fixation rates of the planktonic diatom *Ditylum* were significantly higher

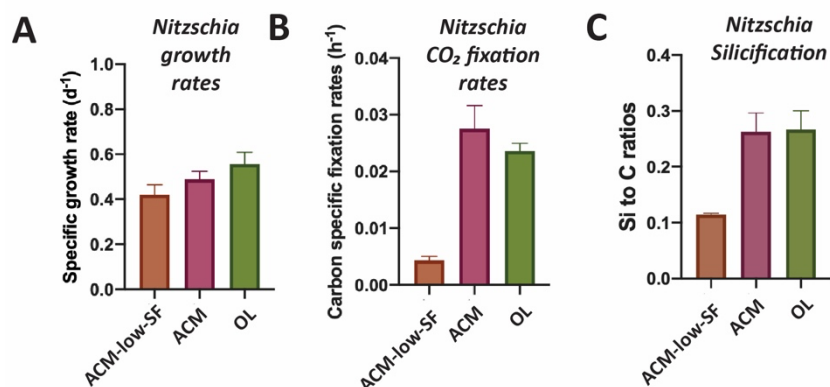


Fig 1. Effects of olivine leachate versus culture medium controls on growth and physiology of the benthic diatom *Nitzschia*. A) Cell-specific growth rates (d⁻¹), B) Carbon-specific fixation rates (hr⁻¹) and C) Si:C ratios (mol:mol) of the benthic diatom *Nitzschia* sp. Abbreviations: OL is olivine leachate, ACM is Aquil control medium, ACM-low-SF is Aquil control medium with lowered Si and Fe concentrations. Values represent the means and error bars are the standard deviations of triplicate cultures for each treatment.

323

324 fixation rates with increasing OL concentrations, with maximum rates observed at and above
325 50% of the original OL (**Fig. 2A, B**). *Ditylum* particulate Si:C ratios also reached levels similar
326 to those seen in the ACM medium in the 80-100% additions (**Fig. 2C**). Likewise, *Ditylum*
327 cellular Fe:P ratios measured by ICP-MS were not significantly different between 100% OL and
328 ACM treatments, suggesting the diatom could access the same amount of Fe from the
329 precipitated Fe(III) in the OL as from the soluble (EDTA-chelated) Fe(III) in the culture medium
330 ($p=0.56$; **Supp. Fig 2A**). These data demonstrate that even at extremely high concentrations,
331 olivine dissolution products including trace metals are not toxic to diatoms, but instead may
332 provide sources of the essential nutrients iron and silicate to support their growth in nutrient
333 replete conditions.

in the OL treatment compared to either the ACM ($p=0.002$; $p=0.0001$) or ACM-low-Si/Fe treatments ($p=0.0002$; $p<0.0001$; **Supp. Fig. 1 A, B**), while Si:C ratios were the same ($p=0.93$; **Supp. Fig 1C**). When *Ditylum* was grown across a range of OL concentrations (i.e., a dilution series from 0% to 100% additions, where 100% corresponds to the OL treatment used in the *Nitzschia* experiment above), we observed increasing growth and CO₂

334 *Coccolithophores*

335 It has been hypothesized that calcifying coccolithophores may benefit from an increase in
 336 alkalinity from olivine dissolution (Bach et al., 2019). In the OL dilution series, maximum
 337 growth rates for the coccolithophore *Emiliana* equivalent to those recorded in the ACM positive

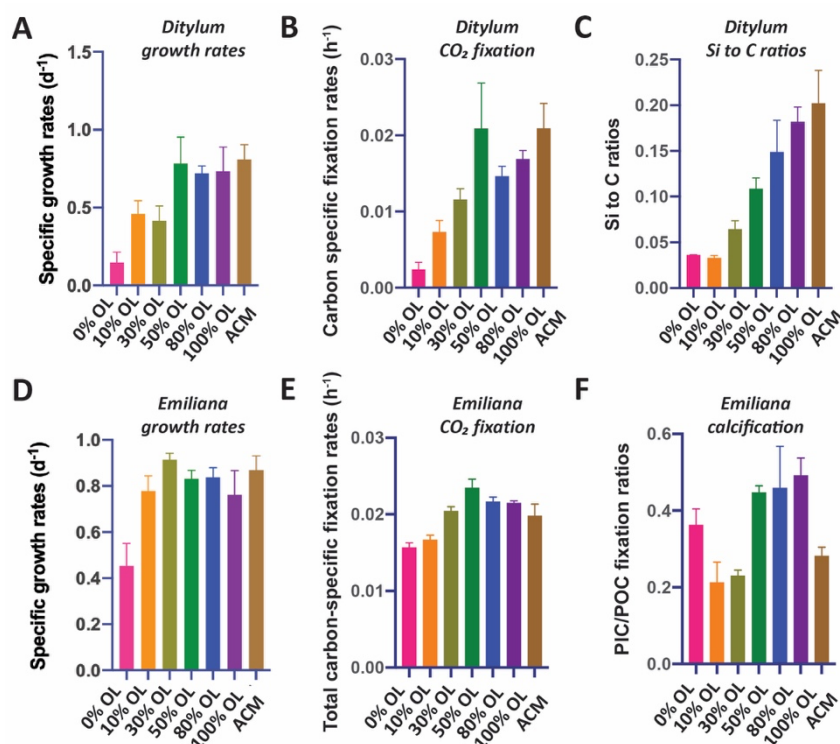


Fig 2. Dilution series of olivine leachate on growth and physiology of a marine diatom and coccolithophore. The diatom *Ditylum* sp. and the coccolithophore *Emiliana huxleyi* were grown across a range of dilutions of the olivine leachate (OL, 0-100%), and in the Aquil control medium (ACM). Shown are: **A)** Cell-specific growth rates (d⁻¹), **B)** Carbon-specific fixation rates (hr⁻¹) and **C)** Si:C ratios (mol:mol) of *Ditylum* sp.. Next, are **D)** Cell-specific growth rates (d⁻¹), **E)** Carbon-specific fixation rates (hr⁻¹), and **F)** PIC production (calcification) rates (hr⁻¹) of *Emiliana huxleyi* in the same OL and ACM treatments. Values represent the means and error bars are the standard deviations of triplicate cultures for each treatment.

338 control medium were achieved at all added OL concentrations from 10% to 100% (**Fig. 2D**). POC production (CO₂ fixation) rates were similar at all OL levels from 30% to 100%, and were not significantly different than in the ACM treatment ($p > 0.05$, **Fig. 2E**). Particulate inorganic carbon to particulate organic carbon fixation ratios (PIC:POC production ratios) were higher at OL levels of 50-100% than in the ACM positive controls (**Fig. 2F**), possibly due to enhanced alkalinity in the high OL concentration treatments.

An independent set of basic two-treatment experiments

366 with the coccolithophore (ACM versus 100% OL, **Supp. Fig 3**) supported the results of the
 367 dilution series experiments shown in **Fig. 2**. *Emiliana* specific growth rates ($p=0.05$), and
 368 cellular particulate inorganic:particulate organic carbon ratios ($p= 0.07$; PIC:POC, mol:mol)
 369 were very similar in the ACM and OL treatments (**Supp. Fig. 3A**). Likewise, POC-specific
 370 fixation rates ($p=0.04$; TC h⁻¹) were slightly higher in the OL than in the ACM treatments, while
 371 PIC:POC fixation ratios were the same ($p=0.07$, **Supp. Fig. 3B**). Similar to diatoms, these data
 372 demonstrate that olivine dissolution products are also not toxic to coccolithophores and that
 373 enhanced alkalinity may support growth in nutrient replete conditions.

374

375 *Cyanobacteria*

376 Like diatoms and coccolithophores, cyanobacteria could benefit from olivine dissolution
377 due to their relatively high Fe (Hutchins and Boyd, 2016) and Ni requirements (Dupont et al.,
378 2008). The OL dilution series experiments using the widely distributed picocyanobacterium
379 *Synechococcus* showed positive responses in growth rates (**Fig. 3A**) and CO₂ fixation rates (**Fig.**
380 **3B**) across the range of OL levels, similar to those of the eukaryotic algae. Both growth rates
381 and carbon fixation rates were the same in the 100% OL treatment as in the ACM positive
382 control treatment (p=0.94; p=0.46). ICP-MS measurements of *Synechococcus* cellular Fe:P
383 ratios across a range of OL levels (0-100%) showed that this isolate accumulated much less Fe in
384 the 0% OL than in the ACM treatment (p=0.02), but in all treatments with added OL, Fe:P ratios
385 were the same as or higher than the ACM values (**Supp. Fig. 2B**). As with the eukaryotic
386 phytoplankton, the synthetic OL provided a good source of Fe to support the growth of the
387 picocyanobacterium.

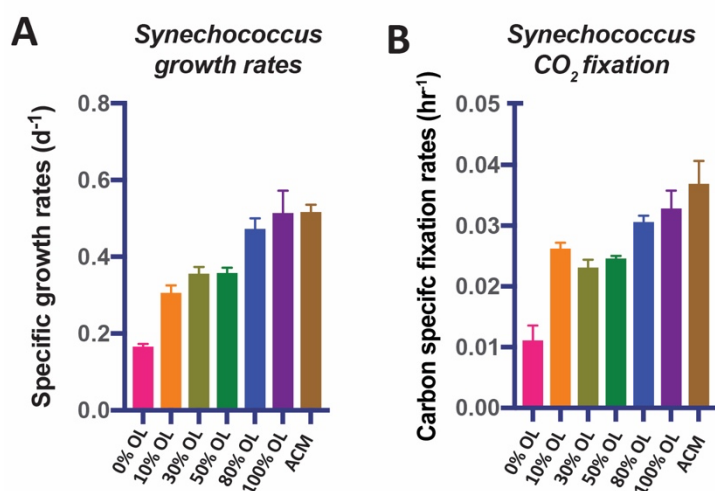


Fig 3. Dilution series of olivine leachate on growth and CO₂ fixation of a marine cyanobacterium. The unicellular picocyanobacterium *Synechococcus* was grown across a range of dilutions of the olivine leachate (OL, 0-100%), and in the Aquil control medium (ACM). Shown are: **A**) Cell-specific growth rates (d⁻¹) and **B**) Carbon-specific fixation rates (hr⁻¹). Values represent the means and error bars are the standard deviations of triplicate cultures for each treatment.

In striking contrast to the eukaryotic algae and the non-diazotrophic (i.e., non-N₂-fixing) picocyanobacterium *Synechococcus*, the N₂-fixing cyanobacterium *Trichodesmium* could not grow at any concentration of OL tested (**Fig. 4A**). One possible explanation for this lack of growth is toxic effects by one of the trace metal components of the OL. We hypothesized that Ni and Co are less likely to be toxic, as these nutrient metals have been found to be relatively non-toxic to phytoplankton at similar environmental concentrations (Guo et al., 2022; Karthikeyan et al., 2019; Panneerselvam et al., 2018). Hence, we hypothesized that Cr toxicity should be considered as a likely

408 possible scenario (Frey et al., 1983; Kiran et al., 2016).

409 Another possibility is that *Trichodesmium* did not experience toxic effects but instead
410 was unable to access Fe from OL. This N₂-fixer requires more Fe than virtually any other
411 phytoplankton species (Hutchins and Sañudo-Wilhelmy, 2021), and the OL was the only source
412 of Fe provided in our experiments. Fe(II) released into seawater from olivine dissolution likely
413 quickly oxidizes to Fe(III), which then precipitates and becomes insoluble at the elevated

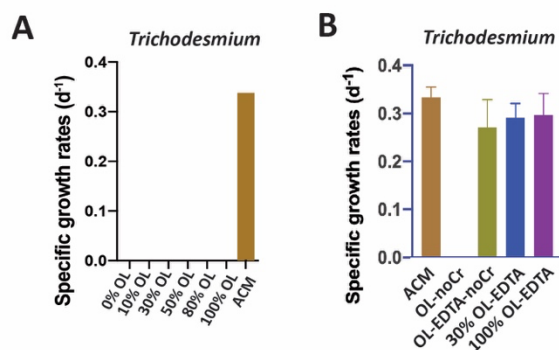


Fig 4. Effects of olivine leachate versus culture medium controls on growth of the marine N₂-fixing cyanobacterium *Trichodesmium*. Shown are **A**) Cell-specific growth rates (d⁻¹) of the colonial cyanobacterium *Trichodesmium* across a range of dilutions of the olivine leachate (OL, 0-100%) and in the Aquil control medium (ACM), and **B**) Cell-specific growth rates (d⁻¹) of *Trichodesmium* in two concentrations of OL (30% and 100%) with the synthetic metal chelator EDTA, and in OL without Cr, or OL without Cr but plus EDTA, versus ACM.

concentrations in our OL (Manck et al., 2022). This could render it biologically unavailable to the cellular Fe uptake systems of some species. We deliberately designed our OL to replicate this oxidation/precipitation process, and as expected observed visible reddish-brown amorphous Fe precipitates on the bottom of the growth flasks for all synthetic OL treatments.

Accordingly, we designed another set of experiments to test for both lack of Fe bioavailability and specific sensitivity to Cr, as has been done in previous cyanobacterial studies (Kiran et al., 2016). To do this, we formulated several variants of the olivine leachate: 1) normal OL (100% concentration), 2) OL (100% concentration) with a synthetic ligand (EDTA) that solubilizes Fe(III), and thus makes it broadly bioavailable (OL-EDTA), 3) OL (100% concentration) but with no Cr (OL-noCr), 4) and OL (100% concentration) but with no Cr and with

434 EDTA (OL-EDTA-noCr) (**Fig. 4B**). *Trichodesmium* also could not grow in the OL medium
435 without added Cr (OL-noCr, **Fig. 4B**), demonstrating that the lack of growth observed in OL
436 was not due to Cr toxicity. However, growth recovered to the same levels as in the ACM when
437 EDTA was added (OL-EDTA) to the leachate (p=0.16; **Fig. 4B**). This suggests that poor
438 bioavailability of the precipitated Fe(III) was the likely cause for *Trichodesmium*'s inability to
439 grow in the unmodified OL.

440 OL also inhibited the growth of the unicellular N₂-fixing cyanobacterium *Crocospaera*,
441 although not to the same extent as for *Trichodesmium*. *Crocospaera* exhibited growth rates that
442 were 22-44% of those in ACM across the full range of OL concentrations, but growth recovered
443 in OL-EDTA to 76% of rates in ACM (**Fig. 5A**). Results were very similar for CO₂ fixation rates
444 and N₂-fixation rates in OL, which were severely reduced by 64-100% (carbon fixation) and 69-
445 88% (N₂ fixation) relative to ACM in all OL treatments, but reached maximum values of 80%
446 and 63% of ACM treatment rates, respectively, when EDTA was added to the OL (**Fig. 5B and**
447 **C**). This demonstrates that oxidized Fe from OL was not effectively utilized to support growth
448 for either of the two N₂-fixing cyanobacteria tested, in contrast to diatoms, coccolithophores, and
449 *Synechococcus*. However, their growth recovery after EDTA additions indicates that the other
450 trace metals Cr, Ni, and Co in the olivine leachate were not toxic, even at extremely high
451 concentrations. Interestingly, unlike *Trichodesmium* which either could not grow at all on OL
452 alone or recovered fully upon EDTA additions, *Crocospaera* could still grow at lower growth
453 rates on OL but could not grow as fast upon EDTA additions as in ACM. Future experiments are

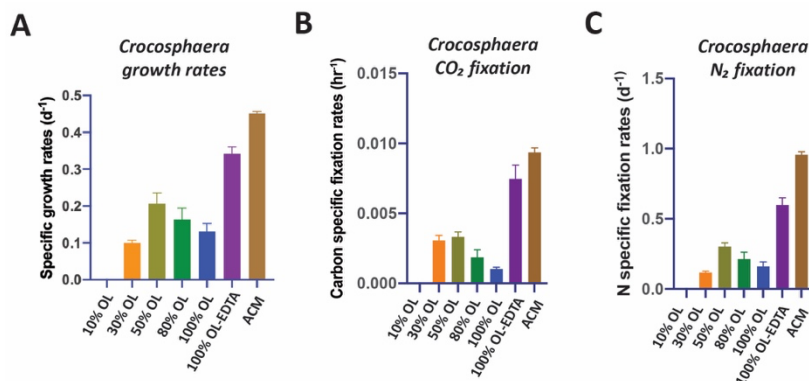


Fig 5. Effects of olivine leachate dilution series versus culture medium controls on the physiology of the marine N₂-fixing cyanobacterium *Crocosphaera*.

A) Cell-specific growth rates (d⁻¹), **B)** Carbon-specific fixation rates (hr⁻¹), and **C)** N-specific fixation rates (day⁻¹) of the unicellular cyanobacterium *Crocosphaera* grown across a range of dilutions of the olivine leachate (OL, 0-100%), in 100% OL plus EDTA (OL-EDTA), and in the Aquil control medium (ACM). Values represent the means and error bars are the standard deviations of triplicate cultures for each treatment.

471

needed to understand these differences in species-specific responses between these two N₂-fixers. Taken together, these data suggest that when olivine dissolves in seawater, it will likely have negligible or no effect (positive or negative) on these cyanobacteria.

Diatom/Coccolithophore Competitive Co-culture

Results of the co-culture, or competition, experiment with the diatom *Ditylum* and the coccolithophore *Emiliania*

472 *huxleyi* are shown in **Fig. 6**. Unlike the semi-continuous experiments shown in the previous
 473 figures, this experiment used closed-system “batch” culturing methods in order to assess and
 474 compare effects on relative biomass accumulation by each species over time. OL (100%
 475 concentration) supported growth of both the diatom (**Fig. 6A**) and the coccolithophore (**Fig. 6B**)
 476 in mixed culture, and biomass was very similar for both species between the OL and ACM
 477 treatments throughout most of the experiment. However, cell yields were higher in the ACM at
 478 the final timepoint for the diatom ($p = 0.009$, **Fig. 6A**). Final cell counts were also higher in the
 479 ACM for the coccolithophore, but this difference was not significant ($p = 0.31$; **Fig. 6B**). Similar
 480 trends were observed when diatom biomass was estimated as biogenic silica (BSi, **Fig. 6C**, p
 481 $= 0.002$) and when coccolithophore biomass was assessed as calcite or particulate inorganic
 482 carbon (PIC, **Fig. 6D**, $p = 0.04$). For the diatom, OL supported growth rates similar to those in
 483 the ACM treatment during the first half of the experiment (**Fig. 6A,C**; **Supp. Fig. 4A**). Growth
 484 rates were also similar in the OL and ACM mediums for the coccolithophore (**Fig. 6B,D**; **Supp.**
 485 **Fig. 4B**). Hence, both phytoplankton groups were able to grow similarly well in co-culture where
 486 each did not exhibit any strong competitive advantage over the other.

487

488

489 Discussion

490

491 In general, simulated olivine dissolution products did not show toxicity even at extremely
 492 high concentrations across all phytoplankton groups, consistent with other recent observations
 493 (Guo et al., 2022). Guo et al. (2022) particularly focused on exposing 11 phytoplankton groups

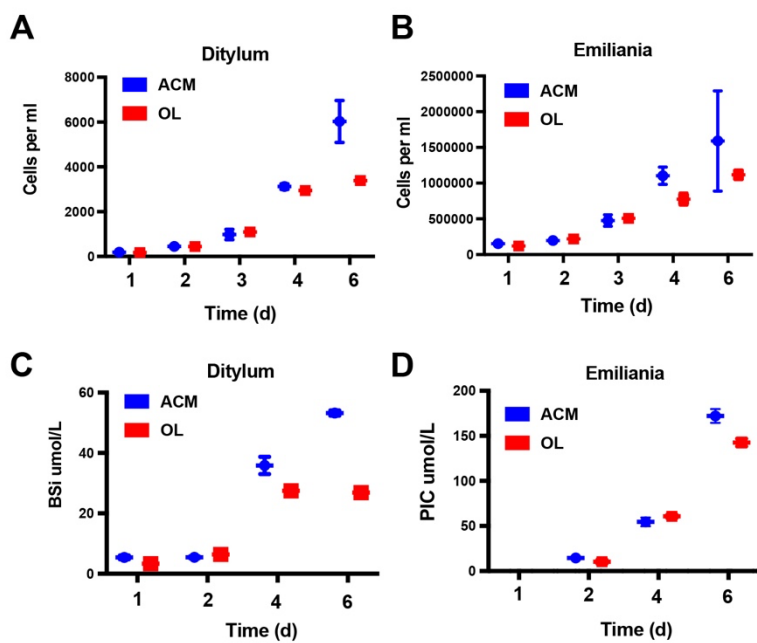


Fig. 6. Effects of olivine leachate versus culture medium controls on growth competition and biomineralization during co-culture of a diatom and a coccolithophore. Shown are 5 day growth curves (cells mL^{-1}) for **A**) the coccolithophore *Emiliana huxleyi* and **B**) the diatom *Ditylum* in mixed cultures grown in olivine leachate (OL, red symbols) and Aquil control medium (ACM, blue symbols). Also shown are **C**) Biogenic silica (BSi, $\mu\text{mol L}^{-1}$), a proxy for diatom biomass, and **D**) Calcite or particulate inorganic carbon (PIC, $\mu\text{mol L}^{-1}$), a proxy for coccolithophore biomass, in the OL and ACM treatments in the same growth competition experiment. Values represent the means and error bars are the standard deviations of triplicate cultures for each treatment.

521 species-specific responses across variations in (0-100 μM) EDTA and Ni (0-50 μM)
 522 concentrations, indicating that specific phytoplankton groups are impacted differently depending
 523 on the chemical species in the total dissolved Ni pools and/or the concentration and type of
 524 organic ligands in seawater. Our results are generally consistent with their overall findings, as the
 525 phytoplankton groups tested here did not exhibit negative effects upon elevated exposure to Ni
 526 with (e.g., ACM) and without added EDTA (e.g., OL), suggesting that Ni was not toxic
 527 irrespective of the concentration of different Ni species in the dissolved pool or that of the Ni^{2+}
 528 ion. However, our experiments were not designed to test for taxon-specific differences in
 529 responses to specific Ni species or variations in EDTA concentrations in particular.

530 Diatoms were able to use synthetic OL-derived Si and Fe to support near-maximum
 531 growth rates and carbon fixation rates, as well as robust silica frustule development; both of
 532 these nutrients can frequently limit diatom growth in various parts of the ocean (Tréguer et al.,
 533 2018; Hutchins and Boyd, 2016). OL-derived alkalinity and iron increases also supported

to elevated Ni concentrations and did not observe strong effects across these taxa. Although it is unknown what chemical species of dissolved Ni primarily influence phytoplankton physiology, most studies indicate that phytoplankton primarily interact with free Ni^{2+} ions but are not particularly sensitive to the total dissolved Ni concentration (Guo et al., 2022). Guo et al. (2022) and our study used the same Ni-containing compound, NiCl_2 , as a source of Ni^{2+} . Guo et al. also used the same base Aquil control medium as our ACM. ACM contains EDTA that binds with metal ions like Ni to improve their dissolution, which subsequently lowers the free Ni ion concentrations (e.g., Ni^{2+}) relative to the total dissolved Ni pool. Although broad negative effects of enhanced Ni concentrations were not observed across taxa, Guo observed some

534 coccolithophore growth, consistent with previous observations in calcifying corals (Albright et
535 al., 2016). Similarly, the globally-distributed picocyanobacterium *Synechococcus* increased its
536 growth and carbon fixation rates as OL concentrations increased. Although OL could not support
537 N₂-fixing cyanobacteria due to their inability to use Fe(III), olivine dissolution products were not
538 observed to be toxic. Their inability to use Fe(III) is a neutral effect due to other sources of
539 bioavailable Fe in the water column (Hutchins and Boyd, 2016). Thus, these results suggest that
540 many phytoplankton will not be negatively impacted by even high levels of elements derived
541 from olivine dissolution, and that some olivine dissolution products may support their growth,
542 primary productivity, and biomineralization when OL is available at high enough concentrations
543 in certain environmental conditions. For example, it is important to note that potential growth
544 benefits to phytoplankton *in situ* will also depend on ambient concentrations of other important
545 nutrients, such as nitrogen (N) and phosphorus (P). Our cultures contained an abundance of other
546 required nutrients, thus enabling phytoplankton to take advantage of particular dissolution
547 products for growth (e.g., Si, Fe, alkalinity). However, if nutrients like N and P are primarily
548 limiting in natural environments, then olivine dissolution products are not expected to have any
549 growth effect. In addition, these cultures represent closed systems that do not allow olivine
550 products to be diluted with fresh seawater. In natural settings, advection in both sediment
551 porewaters (Reimers et al., 2004) and the water column (He and Tyka, 2022) will lead to short
552 residence times, thereby rapidly diluting olivine dissolution products. Hence, these physical
553 dynamics will prevent high concentrations of olivine dissolution products from accumulating in
554 seawater in coastal systems. Thus, even the most dilute leachate treatment in this study is likely
555 more concentrated than the anticipated concentrations of olivine dissolution products expected
556 under field conditions.

557 Bach et al. (2019) (Bach et al., 2019) hypothesized that silicate, iron and nickel releases
558 from marine applications of silicate minerals like olivine might particularly benefit diatoms and
559 cyanobacteria, as these groups have especially high requirements for one or more of these
560 nutrients. Thus, they expected that olivine applications might produce a “Greener” ocean. They
561 also suggested that adding minerals derived from CaCO₃⁻ (such as quicklime applications) would
562 particularly favor coccolithophores, due to rapidly enhanced seawater alkalinity. This outcome
563 would produce a “Whiter” ocean (the color of coccolithophore calcite). Although we did not test
564 CaCO₃⁻ derivatives, our results with synthetic OL seem to point instead to a both “Green and
565 White” ocean, since in individual experiments diatoms, picocyanobacteria, and coccolithophores
566 all responded positively to OL at the relatively elevated levels applied in our experiments. This
567 conclusion is further supported by the results of our diatom/coccolithophore co-culture
568 experiment, which showed that OL stimulated both species simultaneously rather than conferring
569 a competitive advantage on one or the other.

570 Iron in olivine minerals is present as reduced Fe(II), and we added it in this form to our
571 synthetic OL. However, when Fe(II) dissolves in oxic seawater, it quickly (within minutes)
572 oxidizes to highly insoluble Fe(III), which almost entirely precipitates out as amorphous iron
573 oxyhydroxides (Millero et al., 1987). Clearly, in our experiments this oxidized particulate iron

574 must have been available to the species that showed growth enhancement with OL, since no
575 other iron source was provided in the seawater growth medium. Diatoms and some other
576 eukaryotes can access precipitated Fe(III) oxyhydroxides using their well-studied reductive
577 uptake systems (Morrissey and Bowler, 2012), or even potentially through endocytosis in some
578 cases (Kazamia et al., 2018).

579 The responses of the two N₂-fixing cyanobacteria were in striking contrast to those of the
580 other three phytoplankton groups tested. These diazotrophs were either unable to grow in our
581 artificial OL at all (*Trichodesmium*), or could only grow to a very limited degree
582 (*Crocospaera*). Since olivine dissolution products support photoautotrophic growth by other
583 phytoplankton but not diazotrophic growth, this could be taken to indicate that olivine
584 applications might tend to drive the marine ecosystem towards nitrogen limitation, which would
585 limit the upper bound of phytoplankton proliferation. However, our results with experimental
586 additions of the artificial iron chelator EDTA (ethylene diamine tetra acetic acid) suggest that
587 other mechanisms may enable iron bioavailability. For example, previous research has suggested
588 that *Trichodesmium* cannot directly access particulate Fe(III) forms, but likely relies on bacteria
589 residing on and in natural colonies to produce siderophores, which then solubilize particulate
590 Fe(III) sources and make them bioavailable (Rubin et al., 2011; Lee et al., 2018). Since cultured
591 *Trichodesmium* such as ours typically do not produce colonies, but grow instead as individual
592 filaments of cells, cultures of this diazotroph are likely deficient in many of these iron-acquiring
593 microbial symbionts (Rubin et al., 2011). The iron uptake systems of *Crocospaera* have been
594 less well-characterized, but like *Trichodesmium*, molecular studies suggest this unicellular
595 diazotroph lacks the genetic capacity to produce endogenous siderophores (Shi et al., 2010; Yang
596 et al., 2022). Our results show that when we add the artificial iron chelator EDTA (which
597 substitutes for ligands produced by the missing bacteria in cultures), the synthetic OL supports
598 near-maximum growth of both of these diazotrophs. Thus, reduced growth rates of these
599 cyanobacteria in OL without EDTA appear to be due to severe iron limitation, not toxicity of any
600 OL component. In our experiments the cells were forced to grow on OL as a sole source of iron,
601 but in coastal ecosystems where olivine deployments would occur, there are typically many other
602 natural sources of iron to support algal growth (Capone and Hutchins, 2013; Hutchins and Boyd,
603 2016). In nature, *Trichodesmium* is also likely to occur mostly as colonies, and so may have
604 access to additional microbiome-provided iron, including from both naturally-occurring supplies
605 as well as potentially from any shallow-water olivine applications. Thus, iron limitation of N₂
606 fixation due to olivine additions in coastal waters may not occur in the real ocean.

607 Growth inhibition of diazotrophs by our synthetic OL appears to be due to iron limitation,
608 but our experiments also shed light on potential effects of other trace metals present in the
609 formulation. Of the metals found in our synthetic OL, Ni and Co are considered nutrient
610 elements with relatively low toxicity; in fact, the concentrations added even in our maximum
611 dosage experiments were well below those that have been reported to be toxic to phytoplankton
612 (Karthikeyan et al., 2019; Vink and Knops, 2023). However, Cr has the potential to be
613 biologically problematic. Cr(III) found in olivine is relatively insoluble, so in this form it is

614 probably not a major source of exposure for planktonic organisms. However, if it oxidizes to
615 Cr(VI), it becomes much more soluble, and thus more bioavailable and potentially toxic. Cr(III)
616 oxidation is thermodynamically unfavorable, but can be facilitated by borate ions always present
617 in seawater, or by the presence of biologically or photochemically-produced oxidants like H₂O₂
618 (Pettine et al., 1991), and by naturally occurring manganese oxides (Weijden and Reith, 1982).
619 For these reasons, following the principle of “worst case scenario”, we used a soluble Cr(VI) salt
620 in our synthetic OL formulation. Despite this, we found that the presence or absence of the
621 relatively elevated levels of dissolved Cr(VI) present in our regular synthetic OL did not make
622 any difference to the growth of *Trichodesmium* or the other tested phytoplankton species.
623 Particularly, because synthetic OL stimulated near-maximum growth rates in the diatoms,
624 coccolithophore and picocyanobacterium, we presume that the Cr(VI) additions did not
625 adversely affect these groups either.

626 The goal of this work was to test both extreme levels and simultaneous exposure of
627 multiple, biologically important olivine dissolution products that could influence microbial
628 physiology in order to identify thresholds and response curves. Accordingly, our experiments
629 focused on determining acute effects of high concentrations of olivine dissolution products. In
630 general, they suggest that negative impacts may be few even for large olivine deployments, given
631 the high concentrations of tested olivine dissolution products. Because these microplankton serve
632 as important links to higher trophic levels, these data suggest minimal long-term impacts from
633 olivine dissolution on ecosystem services like fisheries. Future research directions may include
634 longer term experiments with prokaryotes and natural microbial communities to expand our
635 understanding of olivine exposure on important taxa that help drive biogeochemical cycling in
636 the oceans. Similar experiments can also be conducted except with other OAE feedstocks
637 harboring different chemical compositions and more rapid dissolution timescales (Renforth and
638 Henderson, 2017). Future studies can also focus on determining how biological processes like
639 photosynthesis, respiration, and organic ligand production could influence olivine dissolution
640 kinetics and their impacts on carbon dioxide removal.

641
642 **Author contribution:** D.A.H., F.-X.F., S.J.R., and N.G.W. designed the research; D.A.H., F.-
643 X.F., S.-C.Y., and S.G.J. performed the research. D.A.H., F.-X.F., S.-C.Y., N.G.W., and S.G.J.
644 analyzed the data. D.A.H., F.-X.F., S.-C.Y., N.G.W., S.J.R., M.G.A., and S.G.J. wrote the paper.

645
646 **Competing interests:** Authors D.A.H. and F.-X.F. received research funding from Vesta, PBC.
647 N.G.W., M.G.A., and S.J.R. are full time employees at Vesta, PBC.

648
649

650

651

652

653

References

654 Albright, R., Caldeira, L., Hosfelt, J., Kwiatkowski, L., Maclaren, J. K., Mason, B. M.,
655 Nebuchina, Y., Ninokawa, A., Pongratz, J., Ricke, K. L., Rivlin, T., Schneider, K., Sesboué, M.,
656 Shamberger, K., Silverman, J., Wolfe, K., Zhu, K., and Caldeira, K.: Reversal of ocean
657 acidification enhances net coral reef calcification, *Nature*, 531, 362–365,
658 <https://doi.org/10.1038/nature17155>, 2016.

659

660 Bach, L. T., Gill, S. J., Rickaby, R. E. M., Gore, S., and Renforth, P.: CO₂ Removal With
661 Enhanced Weathering and Ocean Alkalinity Enhancement: Potential Risks and Co-benefits for
662 Marine Pelagic Ecosystems, *Frontiers in Climate*, 1–21,
663 <https://doi.org/10.3389/fclim.2019.00007>, 2019.

664

665 Beerling, D. J., Kantzas, E. P., Lomas, M. R., Wade, P., Eufrazio, R. M., Renforth, P., Sarkar, B.,
666 Andrews, M. G., James, R. H., Pearce, C. R., Mercure, J.-F., Pollitt, H., Holden, P. B., Edwards,
667 N. R., Khanna, M., Koh, L., Quegan, S., Pidgeon, N. F., Janssens, I. A., Hansen, J., and Banwart,
668 S. A.: Potential for large-scale CO₂ removal via enhanced rock weathering with croplands,
669 *Nature*, 1–20, <https://doi.org/10.1038/s41586-020-2448-9>, 2021.

670

671 Bertrand, E. M., Allen, A. E., Dupont, C. L., Norden-Krichmar, T. M., Bai, J., Valas, R., and
672 Saito, M. A.: Influence of cobalamin scarcity on diatom molecular physiology and identification
673 of a cobalamin acquisition protein, *Proceedings of the National Academy of Sciences*, E1762–
674 E1771, <https://doi.org/10.1073/pnas.1201731109/-/dcsupplemental>, 2012.

675

676 Brzezinski, M. A.: THE Si:C:N RATIO OF MARINE DIATOMS: INTERSPECIFIC
677 VARIABILITY AND THE EFFECT OF SOME ENVIRONMENTAL VARIABLES, *J Phycol*,
678 21, 347–357, <https://doi.org/10.1111/j.0022-3646.1985.00347.x>, 1985.

679

680 Capone, D. G. and Hutchins, D. A.: Microbial biogeochemistry of coastal upwelling regimes in a
681 changing ocean, *Nat Geosci*, 6, 711–717, <https://doi.org/10.1038/ngeo1916>, 2013.

682

683 Dupont, C. L., Barbeau, K., and Palenik, B.: Ni Uptake and Limitation in Marine *Synechococcus*
684 Strains, *Appl Environ Microb*, 74, 23–31, <https://doi.org/10.1128/aem.01007-07>, 2008.

685

686 Field, C., Behrenfeld, M., Randerson, J., and Falkowski, P.: Primary production of the biosphere:
687 integrating terrestrial and oceanic components, *Science*, 281, 237–240, 1998.

- 688
689 Flipkens, G., Blust, R., and Town, R. M.: Deriving Nickel (Ni(II)) and Chromium (Cr(III))
690 Based Environmentally Safe Olivine Guidelines for Coastal Enhanced Silicate Weathering,
691 *Environ Sci Technol*, 55, 12362–12371, <https://doi.org/10.1021/acs.est.1c02974>, 2021.
- 692
693 Frey, B. E., Riedel, G. F., Bass, A. E., and Small, L. F.: Sensitivity of estuarine phytoplankton to
694 hexavalent chromium, *Estuar Coast Shelf Sci*, 17, 181–187, [https://doi.org/10.1016/0272-](https://doi.org/10.1016/0272-7714(83)90062-8)
695 [7714\(83\)90062-8](https://doi.org/10.1016/0272-7714(83)90062-8), 1983.
- 696
697 Fu, F., Zhang, Y., Bell, P. R. F., and Hutchins, D. A.: PHOSPHATE UPTAKE AND GROWTH
698 KINETICS OF *TRICHODESMIUM* (CYANOBACTERIA) ISOLATES FROM THE NORTH
699 ATLANTIC OCEAN AND THE GREAT BARRIER REEF, AUSTRALIA1, *J Phycol*, 41, 62–
700 73, <https://doi.org/10.1111/j.1529-8817.2005.04063.x>, 2005.
- 701
702 Fu, F., Tschitschko, B., Hutchins, D. A., Larsson, M. E., Baker, K. G., McInnes, A., Kahlke, T.,
703 Verma, A., Murray, S. A., and Doblin, M. A.: Temperature variability interacts with mean
704 temperature to influence the predictability of microbial phenotypes, *Global Change Biol*, 28,
705 5741–5754, <https://doi.org/10.1111/gcb.16330>, 2022.
- 706
707 Fu, F.-X., Mulholland, M. R., Garcia, N. S., Beck, A., Bernhardt, P. W., Warner, M. E., Sañudo-
708 Wilhelmy, S. A., and Hutchins, D. A.: Interactions between changing pCO₂, N₂ fixation, and Fe
709 limitation in the marine unicellular cyanobacterium *Crocospaera*, *Limnology and*
710 *Oceanography*, 53, 2472–2484, <https://doi.org/10.4319/lo.2008.53.6.2472>, 2008.
- 711
712 Guo, J. A., Strzepek, R., Willis, A., Ferderer, A., and Bach, L. T.: Investigating the effect of
713 nickel concentration on phytoplankton growth to assess potential side-effects of ocean alkalinity
714 enhancement, *Biogeosciences*, 19, 3683–3697, <https://doi.org/10.5194/bg-19-3683-2022>, 2022.
- 715
716 Hartmann, J., West, A. J., Renforth, P., Köhler, P., Rocha, C. L. D. L., Wolf-Gladrow, D. A.,
717 Dürr, H. H., and Scheffran, J.: ENHANCED CHEMICAL WEATHERING AS A
718 GEOENGINEERING STRATEGY TO REDUCE ATMOSPHERIC CARBON DIOXIDE,
719 SUPPLY NUTRIENTS, AND MITIGATE OCEAN ACIDIFICATION, *Reviews of Geophysics*,
720 1–37, <https://doi.org/10.1002/rog.20004>, 2013.
- 721
722 Hawco, N. J., McIlvin, M. M., Bundy, R. M., Tagliabue, A., Goepfert, T. J., Moran, D. M.,
723 Valentin-Alvarado, L., DiTullio, G. R., and Saito, M. A.: Minimal cobalt metabolism in the

- 724 marine cyanobacterium *Prochlorococcus*, Proc National Acad Sci, 117, 15740–15747,
725 <https://doi.org/10.1073/pnas.2001393117>, 2020.
- 726
- 727 He, J. and Tyka, M. D.: Limits and CO₂ equilibration of near-coast alkalinity enhancement,
728 Egusphere, 2022, 1–26, <https://doi.org/10.5194/egusphere-2022-683>, 2022.
- 729
- 730 Hutchins, D. A. and Boyd, P. W.: Marine phytoplankton and the changing ocean iron cycle,
731 nature climate change, 6, 1072–1079, <https://doi.org/10.1038/nclimate3147>, 2016.
- 732
- 733 Hutchins, D. A. and Sañudo-Wilhelmy, S. A.: The Enzymology of Ocean Global Change, Annu
734 Rev Mar Sci, 14, 1–25, <https://doi.org/10.1146/annurev-marine-032221-084230>, 2021.
- 735
- 736 Hutchins, D. A., Fu, F.-X., Zhang, Y., Warner, M. E., Feng, Y., Portune, K., Bernhardt, P. W.,
737 and Mulholland, M. R.: CO₂ control of *Trichodesmium* N₂ fixation, photosynthesis, growth
738 rates, and elemental ratios: Implications for past, present, and future ocean biogeochemistry,
739 Limnol Oceanogr, 52, 1293–1304, <https://doi.org/10.4319/lo.2007.52.4.1293>, 2007.
- 740
- 741 Jiang, H.-B., Fu, F.-X., Rivero-Calle, S., Levine, N. M., Sañudo-Wilhelmy, S. A., Qu, P.-P.,
742 Wang, X.-W., Pinedo-Gonzalez, P., Zhu, Z., and Hutchins, D. A.: Ocean warming alleviates iron
743 limitation of marine nitrogen fixation, Nat Clim Change, 8, 709–712,
744 <https://doi.org/10.1038/s41558-018-0216-8>, 2018.
- 745
- 746 John, S. G., Kelly, R. L., Bian, X., Fu, F., Smith, M. I., Lanning, N. T., Liang, H., Pasquier, B.,
747 Seelen, E. A., Holzer, M., Wasylenki, L., Conway, T. M., Fitzsimmons, J. N., Hutchins, D. A.,
748 and Yang, S.-C.: The biogeochemical balance of oceanic nickel cycling, Nat Geosci, 15, 906–
749 912, <https://doi.org/10.1038/s41561-022-01045-7>, 2022.
- 750
- 751 Karthikeyan, P., Marigoudar, S. R., Nagarjuna, A., and Sharma, K. V.: Toxicity assessment of
752 cobalt and selenium on marine diatoms and copepods, Environ Chem Ecotoxicol, 1, 36–42,
753 <https://doi.org/10.1016/j.eneco.2019.06.001>, 2019.
- 754
- 755 Kazamia, E., Sutak, R., Paz-Yepes, J., Dorrell, R. G., Vieira, F. R. J., Mach, J., Morrissey, J.,
756 Leon, S., Lam, F., Pelletier, E., Camadro, J.-M., Bowler, C., and Lesuisse, E.: Endocytosis-
757 mediated siderophore uptake as a strategy for Fe acquisition in diatoms, Sci Adv, 4, eaar4536,
758 <https://doi.org/10.1126/sciadv.aar4536>, 2018.

- 759
760 Kiran, B., Rani, N., and Kaushik, A.: Environmental toxicity: Exposure and impact of chromium
761 on cyanobacterial species, *J Environ Chem Eng*, 4, 4137–4142,
762 <https://doi.org/10.1016/j.jece.2016.09.021>, 2016.
- 763
764 Kling, J. D., Kelly, K. J., Pei, S., Rynearson, T. A., and Hutchins, D. A.: Irradiance modulates
765 thermal niche in a previously undescribed low-light and cold-adapted nano-diatom, *Limnol*
766 *Oceanogr*, 66, 2266–2277, <https://doi.org/10.1002/lno.11752>, 2021.
- 767
768 Lee, M. D., Webb, E. A., Walworth, N. G., Fu, F.-X., Held, N. A., Saito, M. A., and Hutchins,
769 D. A.: Transcriptional Activities of the Microbial Consortium Living with the Marine Nitrogen-
770 Fixing Cyanobacterium *Trichodesmium* Reveal Potential Roles in Community-Level Nitrogen
771 Cycling, *Applied and environmental microbiology*, 84, e02026-17–16,
772 <https://doi.org/10.1128/aem.02026-17>, 2018.
- 773
774 Manck, L. E., Park, J., Tully, B. J., Poire, A. M., Bundy, R. M., Dupont, C. L., and Barbeau, K.
775 A.: Petrobactin, a siderophore produced by *Alteromonas*, mediates community iron acquisition in
776 the global ocean, *Isme J*, 16, 358–369, <https://doi.org/10.1038/s41396-021-01065-y>, 2022.
- 777
778 Meysman, F. J. R. and Montserrat, F.: Negative CO₂ emissions via enhanced silicate weathering
779 in coastal environments, *Biol Letters*, 13, 20160905, <https://doi.org/10.1098/rsbl.2016.0905>,
780 2017.
- 781
782 Millero, F. J., Sotolongo, S., and Izaguirre, M.: The oxidation kinetics of Fe(II) in seawater,
783 *Geochim Cosmochim Ac*, 51, 793–801, [https://doi.org/10.1016/0016-7037\(87\)90093-7](https://doi.org/10.1016/0016-7037(87)90093-7), 1987.
- 784 Moran, M. A.: The global ocean microbiome, *Science*, 350, aac8455–aac8455,
785 <https://doi.org/10.1126/science.aac8455>, 2015.
- 786
787 Morrissey, J. M. and Bowler, C.: Iron utilization in marine cyanobacteria and eukaryotic algae,
788 *Frontiers in Microbiology*, 3, 1–13, <https://doi.org/10.3389/fmicb.2012.00043/abstract>, 2012.
- 789
790 Paasche, E., Brubak, S., Skattebøl, S., Young, J. R., and Green, J. C.: Growth and calcification in
791 the coccolithophorid *Emiliania huxleyi* (Haptophyceae) at low salinities, *Phycologia*, 35, 394–
792 403, <https://doi.org/10.2216/i0031-8884-35-5-394.1>, 1996.
- 793

- 794
795 Panneerselvam, K., Marigoudar, S. R., and Dhandapani, M.: Toxicity of Nickel on the Selected
796 Species of Marine Diatoms and Copepods, *Bull. Environ. Contam. Toxicol.*, 100, 331–337,
797 <https://doi.org/10.1007/s00128-018-2279-7>, 2018.
- 798
799 Pettine, M., Millero, F. J., and Noce, T. L.: Chromium (III) interactions in seawater through its
800 oxidation kinetics, *Mar Chem*, 34, 29–46, [https://doi.org/10.1016/0304-4203\(91\)90012-1](https://doi.org/10.1016/0304-4203(91)90012-1), 1991.
- 801
802 Reimers, C. E., Stecher, H. A., Taghon, G. L., Fuller, C. M., Huettel, M., Rusch, A., Ryckelynck,
803 N., and Wild, C.: In situ measurements of advective solute transport in permeable shelf sands,
804 *Cont Shelf Res*, 24, 183–201, <https://doi.org/10.1016/j.csr.2003.10.005>, 2004.
- 805
806 Renforth, P. and Henderson, G.: Assessing ocean alkalinity for carbon sequestration, *Rev*
807 *Geophys*, 55, 636–674, <https://doi.org/10.1002/2016rg000533>, 2017.
- 808
809 Rimstidt, J. D., Brantley, S. L., and Olsen, A. A.: Systematic review of forsterite dissolution rate
810 data, *Geochim Cosmochim Acta*, 99, 159–178, <https://doi.org/10.1016/j.gca.2012.09.019>, 2012.
- 811
812 Rubin, M., Berman-Frank, I., and Shaked, Y.: Dust- and mineral-iron utilization by the marine
813 dinitrogen-fixer *Trichodesmium*, *Nature Geoscience*, 4, 529–534,
814 <https://doi.org/10.1038/ngeo1181>, 2011.
- 815
816 Shi, T., Ilikchyan, I., Rabouille, S., and Zehr, J. P.: Genome-wide analysis of diel gene
817 expression in the unicellular N₂-fixing cyanobacterium *Crocospaera watsonii* WH 8501, *Isme*
818 *J*, 4, 621–632, <https://doi.org/10.1038/ismej.2009.148>, 2010.
- 819
820 Sunda, W. G. and Huntsman, S. A.: Cobalt and zinc interreplacement in marine phytoplankton:
821 Biological and geochemical implications, *Limnol Oceanogr*, 40, 1404–1417,
822 <https://doi.org/10.4319/lo.1995.40.8.1404>, 1995.
- 823
824 Sunda, W. G., Price, N. M., and Morel, F. M. M.: Trace Metal Ion Buffers and Their Use in
825 Culture Studies, *Algal Culturing Techniques*, 35–63, [https://doi.org/10.1016/b978-012088426-](https://doi.org/10.1016/b978-012088426-1/50005-6)
826 [1/50005-6](https://doi.org/10.1016/b978-012088426-1/50005-6), 2005.
- 827
828 Tovar-Sanchez, A., Sañudo-Wilhelmy, S. A., Garcia-Vargas, M., Weaver, R. S., Popels, L. C.,

829 and Hutchins, D. A.: A trace metal clean reagent to remove surface-bound iron from marine
830 phytoplankton, *Mar Chem*, 82, 91–99, [https://doi.org/10.1016/s0304-4203\(03\)00054-9](https://doi.org/10.1016/s0304-4203(03)00054-9), 2003.

831
832 Tréguer, P., Bowler, C., Moriceau, B., Dutkiewicz, S., Gehlen, M., Aumont, O., Bittner, L.,
833 Dugdale, R., Finkel, Z., Iudicone, D., Jahn, O., Guidi, L., Lasbleiz, M., Leblanc, K., Levy, M.,
834 and Pondaven, P.: Influence of diatom diversity on the ocean biological carbon pump, *Nat*
835 *Geosci*, 11, 27–37, <https://doi.org/10.1038/s41561-017-0028-x>, 2018.

836
837 Vink, J. P. M. and Knops, P.: Size-Fractionated Weathering of Olivine, Its CO₂-Sequestration
838 Rate, and Ecotoxicological Risk Assessment of Nickel Release, *Mineral-basel*, 13, 235,
839 <https://doi.org/10.3390/min13020235>, 2023.

840
841 Weijden, C. H. V. D. and Reith, M.: Chromium(III) — chromium(VI) interconversions in
842 seawater, *Mar Chem*, 11, 565–572, [https://doi.org/10.1016/0304-4203\(82\)90003-2](https://doi.org/10.1016/0304-4203(82)90003-2), 1982.
843 Welschmeyer, N. A.: Fluorometric analysis of chlorophyll a in the presence of chlorophyll b and
844 pheopigments, *Limnol Oceanogr*, 39, 1985–1992, <https://doi.org/10.4319/lo.1994.39.8.1985>,
845 1994.

846
847 Yamamoto, T., Goto, I., Kawaguchi, O., Minagawa, K., Ariyoshi, E., and Matsuda, O.:
848 Phytoremediation of shallow organically enriched marine sediments using benthic microalgae,
849 *Mar Pollut Bull*, 57, 108–115, <https://doi.org/10.1016/j.marpolbul.2007.10.006>, 2008.

850
851 Yang, N., Lin, Y.-A., Merkel, C. A., DeMers, M. A., Qu, P.-P., Webb, E. A., Fu, F.-X., and
852 Hutchins, D. A.: Molecular mechanisms underlying iron and phosphorus co-limitation responses
853 in the nitrogen-fixing cyanobacterium *Crocospaera*, *Isme J*, 16, 2702–2711,
854 <https://doi.org/10.1038/s41396-022-01307-7>, 2022.

855